Nonlinear Dynamics **27:** 185–195, 2002.

Type-I Intermittency and Crisis-Induced Intermittency in a Semiconductor Laser under Injection Current Modulation

E. F. MANFFRA* and I. L. CALDAS
Instituto de Física, Universidade de São Paulo, Caixa Postal 66318, 05315–970 São Paulo SP, Brazil

R. L. VIANA
Departamento de Física, Universidade Federal do Paraná, Caixa Postal 19081, 81531-990 Curitiba PR, Brazil

H. J. KALINOWSKI
CPGEI, Centro Federal de Educação Tecnológica do Paraná, 80230-901 Curitiba PR, Brazil

(Received: 25 July 2000; accepted: 27 March 2001)

Abstract. The dynamics of a negative gain suppression factor laser diode subjected to injection current modulation is similar to that of a damped nonlinear oscillator under periodic forcing. Quasi-periodicity, frequency locking and chaos may be present, depending on the values of the forcing parameters. We have found, for some parameter values, type-I intermittent behavior and crisis-induced intermittency. Scaling laws were obtained for the duration of the laminar phase and the chaos-chaos switchings, respectively. The scale exponents are very close to those expected for one-dimensional unimodal maps.

Keywords: Intermittency, crisis, chaos, diode, lasers, Lyapunov plots.

The study of the dynamical properties of semiconductor lasers is essential for determining their performance as light sources in optical communication systems. Due to nonlinearities always present in laser systems [1], chaos has been detected experimentally and predicted theoretically in different types of semiconductor lasers [2, 3]. Of special relevance are semiconductor lasers with wavelength constraints, such as VCSELs (vertical cavity surface emmiting lasers) and DFBs (distributed feedback lasers), since their single mode operation is a requirement in long distance high speed optical communication systems. In these lasers, the constraints may give rise to a negative gain suppression factor [4], which was shown to be related to self-pulsation even under steady injection current [5]. It has been also suggested that, when the self-pulsating laser is submitted to injection current modulation, it may exhibit quasi-periodicity, frequency locking and chaos. Chaotic optical waveforms can be used to communicate masked information at high bandwidths [6].

In the present note we have analyzed some of the effects of injection current modulation on the dynamics of a self-pulsating laser diode. We have obtained Lyapunov plots of the modulation parameter space (considering the amplitude and frequency of external periodic forcing) and observed, in a certain portion of it, a similarity between its structure and that of a one-dimensional sine-circle map [7]. We have located the corresponding Arnol'd tongues

* Present address: Max-Planck-Institut für Physik Komplexer Systeme, Noethnitzer Str. 38, 01187 Dresden, Germany

Table 1. Values of the physical quantities for the semiconductor laser model.

Parameter	Value
τ_n	1.49 ns
τ_p	3.89 ps
α	1.58×10^{-35} A.m^3.s
Γ	0.986
β	1.0×10^{-5}
N_t	9.26×10^{23} m^{-3}
γ	8.69×10^{-13} s^{-1}.m^3
ε	-2.2×10^{-23} m^{-3}

in the parameter space, and observed other interesting features such as super-stable lines, resonance intersections related to multi-stable behavior, and the existence of a critical line where the resonance regions start to overlap, and above which chaotic behavior may occur.

In addition, we have described routes to chaos exhibited by the laser diode model as the modulation amplitude is varied. Quasi-periodicity is followed by mode-locking (via tangent bifurcation) and then by a period-doubling cascade to chaos when the modulation amplitude is increased. After the accumulation point of those bifurcations there is a sequence of periodic windows and band-merging crisis very similar to that observed in unimodal maps [8]. We have studied the scaling of typical average lengths in the intermittent time series related to band-merging crisis and tangent bifurcations, and observed that the exponents obtained are very close to the values expected for one-dimensional unimodal maps. This is a quantitative evidence that the system dynamics can be well described by those maps in a great extent of the modulation parameter space.

The dynamics of the laser diode model with injection current studied here is modeled by the following single mode rate equations [5]:

$$\frac{\mathrm{d}N}{\mathrm{d}\tau'} = \frac{1}{\alpha} I(\tau') - \gamma(N - N_t)(1 - \varepsilon S)S - \frac{1}{\tau_n} N, \tag{1}$$

$$\frac{\mathrm{d}S}{\mathrm{d}\tau'} = \Gamma\gamma(N - N_t)(1 - \varepsilon S)S - \frac{1}{\tau_p} S + \frac{1}{\tau_n}\Gamma\beta N, \tag{2}$$

where S and N are, respectively, the photon and carrier densities, τ' is the physical time and I is the injected current in the active region. The product of the active region volume and the electronic charge is denoted by α, Γ is the mode confinement factor, β stands for the fraction of spontaneous emission in the lasing mode, N_t is the carrier density required for transparency, and γ is the optical gain coefficient. The gain suppression factor is denoted by ε, which has a negative value due to the wavelength constraints of this semiconductor laser model [4], whereas τ_n and τ_p are the carrier and photon lifetimes, respectively. The values for these parameters we use in the numerical simulations shown in this paper are given in Table 1.

We define reduced photon and carrier densities

$$x_1 = |\varepsilon| N, \quad x_2 = |\varepsilon| S, \tag{3}$$

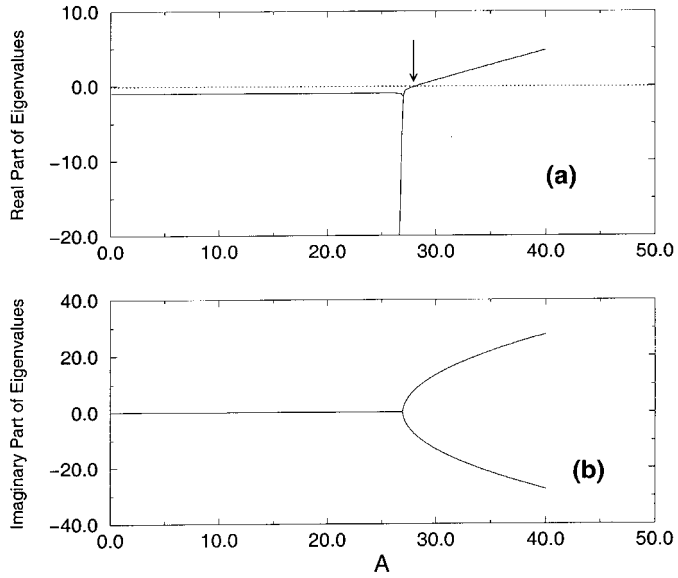

Figure 1. Dependence of (a) the real part, and (b) the imaginary part of the eigenvalues for the linearized system, on the steady injection current A. The arrow indicates the point where a supercritical Hopf bifurcation occurs.

as well as a non-dimensional time $t = \tau'/\tau_n$. The physical constants can also be suitably arranged to get normalized quantities

$$J(t) = \frac{I(t)\tau_n|\varepsilon|}{\alpha}, \quad C = \frac{\gamma\tau_n}{|\varepsilon|}, \quad D = |\varepsilon|N_t, \tag{4}$$

$$E = \frac{\tau_n}{\tau_p}, \quad F = \Gamma\beta, \quad G = \frac{\varepsilon}{|\varepsilon|} = -1, \quad H = \Gamma D, \tag{5}$$

so that we can rewrite the rate equations (1) and (2) in a normalized form

$$\frac{\mathrm{d}x_1}{\mathrm{d}t} = J(t) - x_1 - C(x_1 - D)(1 - Gx_2)x_2, \tag{6}$$

$$\frac{\mathrm{d}x_2}{\mathrm{d}t} = Fx_1 - Ex_2 + H(x_1 - D)(1 - Gx_2)x_2. \tag{7}$$

A linear stability analysis of Equations (6) and (7) for steady injection $J = A$ shows that there is a stable equilibrium point for sufficiently low injection current values, characterizing a steady state for laser operation. This state undergoes a supercritical Hopf bifurcation at a threshold current value, as have been pointed out by Bennett et al. [5]. In Figure 1, we illustrate this transition as we vary the steady injection current $J = A$, showing the real and imaginary parts of the Jacobian matrix eigenvalues for the flow (6, 7). The threshold of self pulsation occurs at $A \approx 28.21$, where there is a supercritical Hopf bifurcation characterized by the emergence of a stable limit cycle, the equilibrium point becoming unstable. We adopt the value $A = 40.44$ in the subsequent analyses. An example of limit cycle is depicted in Figure 2, in which we have a frequency (hereby denoted W_0) numerically found to be equal to 11.70 (corresponding physically to a 1.25 GHz oscillation).

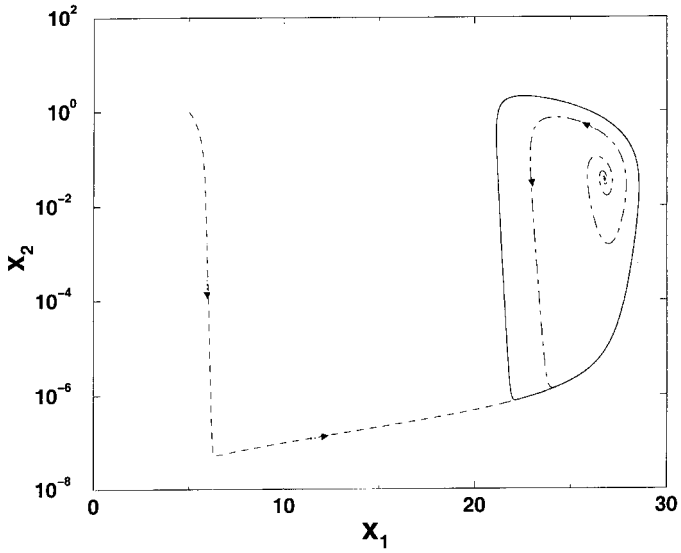

Figure 2. Limit cycle in the phase plane (x_1, x_2) for $A = 40.44$. Dotted lines represent two trajectories, starting from different initial conditions, that asymptote to the limit cycle.

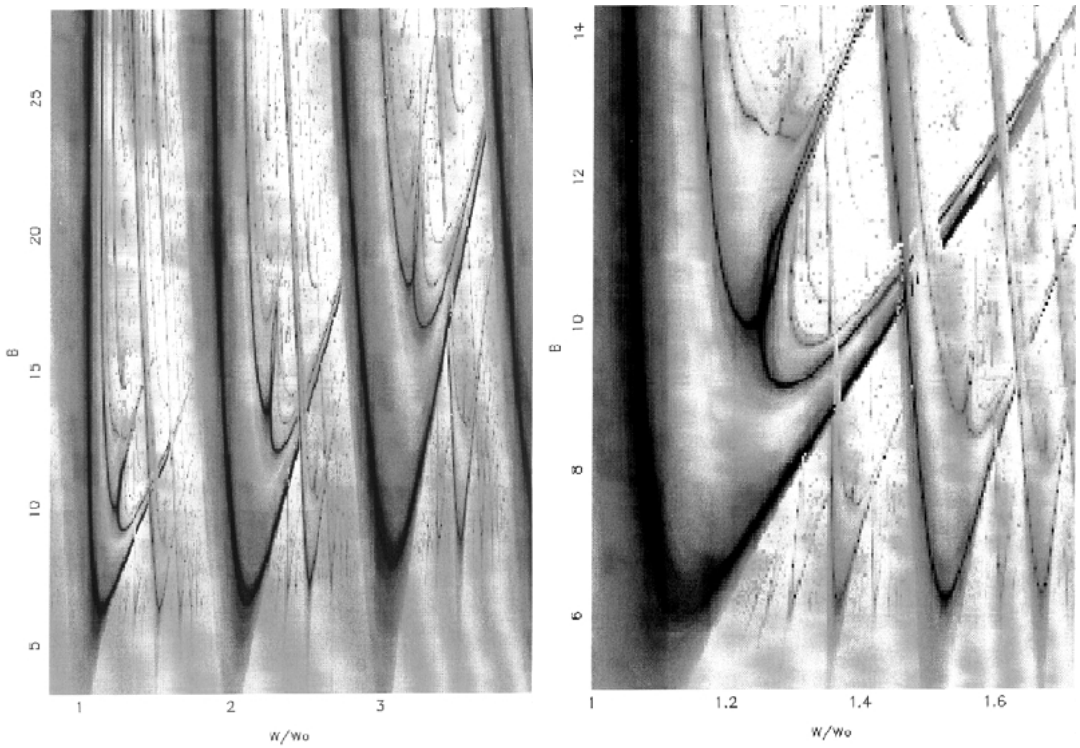

Figure 3. (a) Lyapunov plot of the modulation parameter space. The maximal exponent is represented in grayscale, for which the larger the exponent, the brighter is the pixel in the figure. (b) Enlargement of a region of the Lyapunov plot of the modulation parameter space.

When a sinusoidal time modulation is added to the steady injection current in the form $J(t) = A + B\sin(Wt)$, the system behaves like a periodically driven nonlinear oscillator. Therefore, it can exhibit quasi-periodic motion, frequency locking, and chaos depending on the values of B and W. In order to identify these dynamical regimes in the modulation parameter space (W *versus* B), we have shown in Figures 3a and 3b two Lyapunov plots, on which the largest Lyapunov exponent is represented by gray-scale. The Lyapunov exponents were computed according to the Eckmann–Ruelle algorithm [9]. The second exponent was observed to remain between -55 and -80, indicating a strongly dissipative system. We can identify frequency locking regions (Arnol'd tongues), and supercritical lines (darker lines inside the tongues) that correspond to periodic super-stable orbits for which the Lyapunov exponent diverges. Between each pair of Arnol'd tongues we have regions of quasi-periodic behavior, as evidenced by the vanishing of the maximal Lyapunov exponent.

It is possible to identify a critical line at $B \approx 6.0$ touching the tips of all main super-stable lines (see Figure 3a). This critical line divides the parameter space into two distinct regions: below it only quasi-periodic and mode-locked attractors are observed, and above it period doubling cascades and chaotic attractors may be observed [10]. Above the critical line, the tongues typically develop two branches and intersections of branches belonging to different tongues occur. These intersections are commonly related with coexistence of attractors and multi-stability. In the intersection regions the system may evolve to any of the possibly coexisting attractors depending on the initial condition chosen. Taking this fact into account, we have always used the same initial conditions, namely $x_1 = x_2 = 0$. A larger region of the parameter space is shown in Figure 4 and it is possible to observe that main tongues associated to periods one, two, three, etc. grow up from those points where $(W/W_0) = 1, 2, 3, \ldots$. The overall structure near these tongues is the same as for the first tongue (see Figure 3b). Note also that the critical line for larger W is no longer at a fixed value of $B \approx 6.0$ but goes upward with increasing W. The general features observed in the parameter space of this system are very similar to those found in circle maps [7]. It is indeed possible to derive analytically such maps from a class of impulsively forced limit-cycle oscillators [11].

In order to clarify this connection with one-dimensional circle maps, in Figure 4 we depict first return maps for three different points of the parameter space of Figure 3. The first corresponds to the border of the period-1 Arnol'd tongue (Figure 4a). There is a quadratic tangency of the return map with the 45°-line, pointing out that a tangent bifurcation takes place on the border of the tongue. The second and third return maps depicted in Figures 4b and 4c correspond to points in the parameter space chosen next to a region of chaotic motion near the period-1 tongue, respectively. The latter map has a unimodal character.

In order to reveal other routes to chaotic behavior exhibited by this model we considered in Figure 5a a bifurcation diagram for the normalized photon density x_1, obtained by keeping W constant at $3.2W_0$ and varying B over the range $0.0 < B < 40.0$. For B values up to approximately 8.0, the system exhibits quasi-periodic behavior, as shown in Figure 5b by the vanishing of the maximal Lyapunov exponent. After a tangent bifurcation, as the value of B is further increased, the interior of an Arnol'd tongue is reached, and the dynamics is locked in a period-3 orbit. Following this orbit, a period-doubling bifurcation cascade leads the system to undergo chaotic motion.

The sequence of periodic windows and chaotic band mergings is similar to that of unimodal maps, what may be seen in Figure 5c, where a part of the bifurcation diagram depicted in Figure 5a has been magnified. We may see in any of the three chaotic bands a period-6 window between the points indicated by the symbols $B4$ and $B2$ (that will be related to

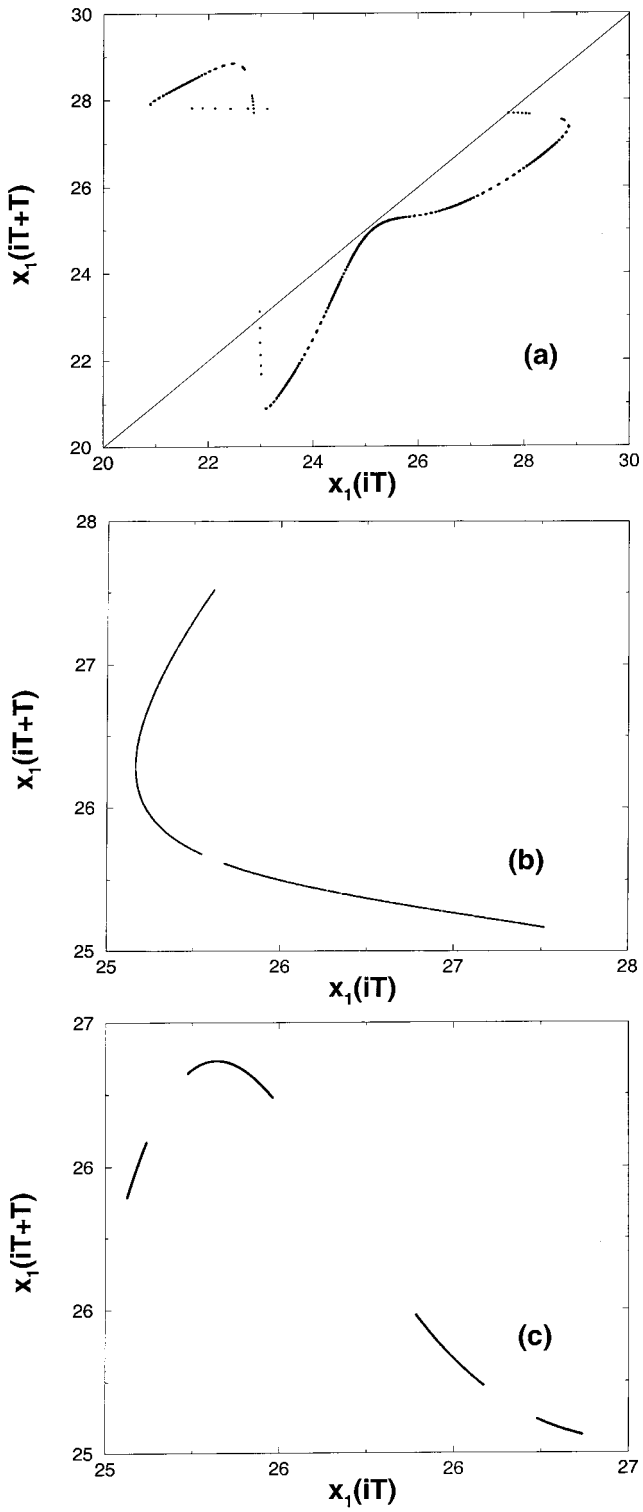

Figure 4. First return maps for selected values of the modulation frequency and amplitude: (a) $W = 1.2W_0$, $B = 5.8$; (b) $W = 1.2W_0$, $B = 16.6$; (c) $W = 1.3W_0$, $B = 10.2$.

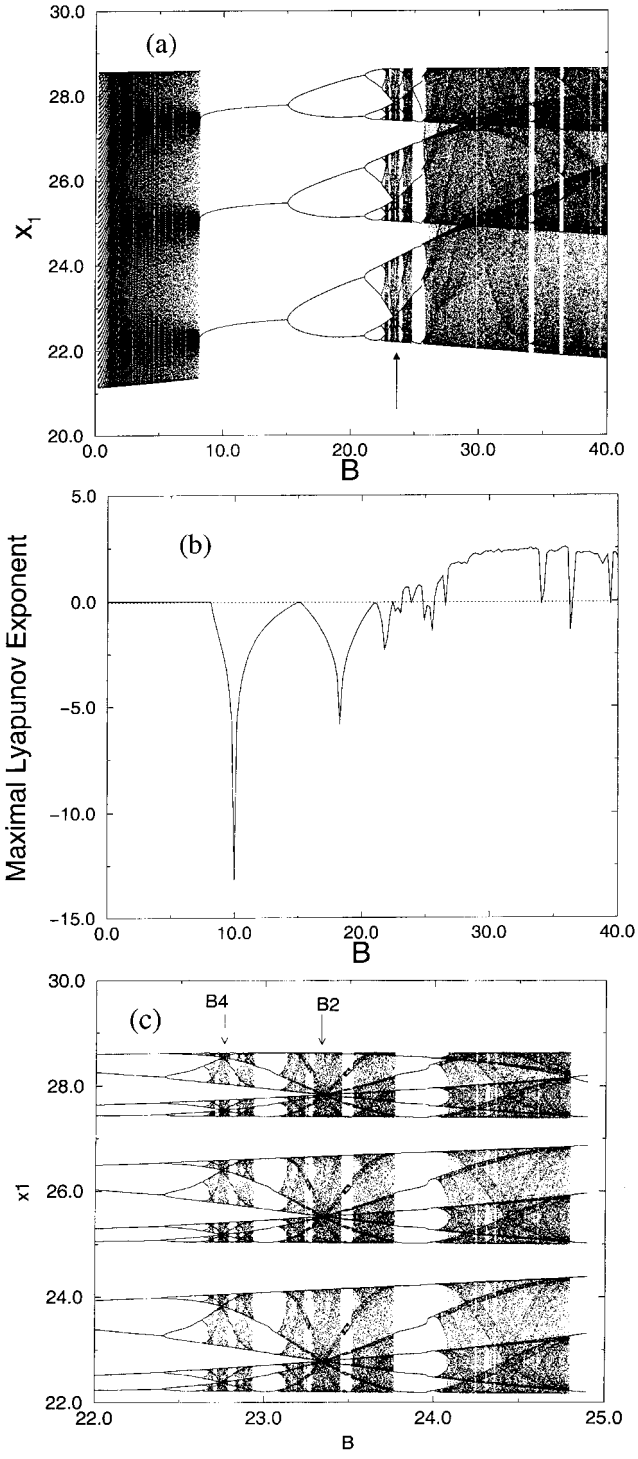

Figure 5. (a) Bifurcation diagram for x_1 *versus* amplitude modulation B, with $W = 3.2W$; (b) maximal Lyapunov exponent; (c) enlargement of a region of (a) indicated by an arrow. Band merging crises are indicated by arrows as B_2 and B_4.

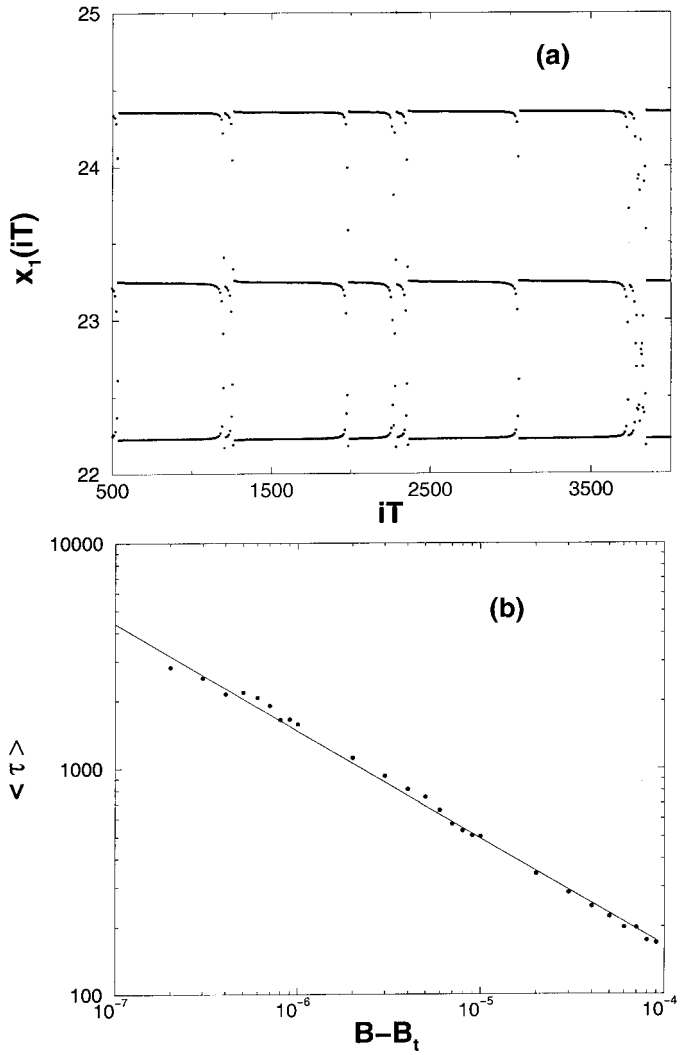

Figure 6. (a) Time series for the stroboscopic map of x_1 with $W = 3.2W_0$ and $B = 24.785$ (only the lower branch is shown). (b) Average duration of the laminar phase as a function of the difference $B - B_t$, near the tangent bifurcation value ($B_t \approx 24.780$).

critical behavior later on). In the right side of $B2$ we can observe a period-7 and a period-5 windows, whereas a period-3 windows is in the extreme right side of the diagram. In some of the observed periodic windows we find bubbles with brief period doubling sequences followed by similar but reverse sequences; as for $B \approx 23.5$, for example (see Figure 5c). This ordering of periodic windows embedded in the chaotic region is in accordance with the U-sequence [12], what emphasizes the connection of the behavior of this laser diode model with injected current modulation with that of a uni-dimensional circle map.

We observe the existence of intermittent behavior in many points of the bifurcation diagram, where a chaotic region suddenly disappears, and a tangent bifurcation gives rise to a periodic window [13]. Note that the period-3 orbit starting at $B \approx 8.0$ in Figure 5a does not come from an intermittent transition, since for $B \lesssim 8.0$ the dynamics is quasi-periodic, rather than chaotic. For example, let us consider the time series for the stroboscopic (time-

$2\pi/W$) map when B is near a period-9 window (Figure 6a). Only the part corresponding to the lower branch in the bifurcation diagram is shown for simplicity. We observe the characteristic features of type-I intermittency scenario: the system remains near the period nine orbit for long stretches of time and escapes from it during the chaotic bursts, before being re-injected in the vicinity of that orbit. We have computed the average time $\langle\tau\rangle$ an orbit stays in the laminar phase, considering a large number of initial conditions in the phase plane. This average laminar duration depends on the B parameter in a power-law fashion, when B approaches B_t

$$\langle\tau\rangle \sim k(B - B_t)^{\gamma}, \tag{8}$$

where $B_t \approx 24.78$ is the value of the tangent bifurcation parameter, at the border of a period-9 window. We have found (see Figure 6b) that $\gamma = 0.474 \pm 0.007$, where the deviation is related to the linear regression procedure. This result is very close to $\gamma = 0.5$, which is the value theoretically predicted for unimodal quadratic maps [13].

Another dynamical feature observed in this model was crisis-induced intermittency, which typically follows an interior crisis, in the same way that a chaotic transient follows a boundary crisis. An interior crisis occurs when a chaotic attractor collides, in the state space, with an unstable periodic orbit, as a system parameter is varied through a critical value. This collision turns the former chaotic attractor into a chaotic saddle, a non-attracting dense chaotic set [14]. This behavior is typically present in mergings of chaotic bands in bifurcation diagrams. Just after an interior crisis, the orbit spends long periods of time bouncing in the region to which the attractor was restricted before the crisis. After one of these long irregular oscillations the orbit escapes from this region and wanders erratically through a new and enlarged region that was made possible for the orbit after a crisis has been occurred. The orbit eventually returns to the former chaotic region to which it was restricted to move, yielding chaos-chaos transitions which are found to obey a power-law scaling for the average time between two successive chaos-chaos switchings [15].

Let $\langle\tau\rangle$ correspond to the average time between two consecutive switchings, for a parameter value slightly above some band-merging crisis parameter (see Figure 7a). The two values of crisis parameters used to analyze this chaos-chaos crisis-induced intermittency were labeled as B_4 and B_2 in the bifurcation diagram of Figure 5c. A scaling law similar to Equation (8) was obtained for $\langle\tau\rangle$, the corresponding exponent (γ) being equal to 0.493 ± 0.015 for the transition near B_4, and 0.498 ± 0.004 for B_2 (see Figure 7b). These values are still in good accordance with the theoretical value of 0.5 predicted for one-dimensional quadratic maps [8]. From the symmetries presented in the parameter space (see Figure 3) one could imagine that routes to chaos similar to those described above are typical for this system. Indeed, the bifurcation diagrams in the vicinity of other main tongues are very similar to the one shown in this note, the main diference being the number of branches, the motion inside each branch being quite similar.

In summary, we have analyzed the dynamics of a self-pulsating laser diode model under injection current modulation. Using Lyapunov plots in the modulation parameter space we have found many similarities between the laser model dynamics and that exhibited by a one-dimensional circle map. We have observed super-stable lines in the parameter space, which correspond to periodic motions less sensitive to external noise, and hence of practical interest. The bifurcation diagram obtaining by varying the injected current amplitude is very similar to that of a unimodal map. In particular, we have observed an ordering of period windows in accordance with the U-sequence.

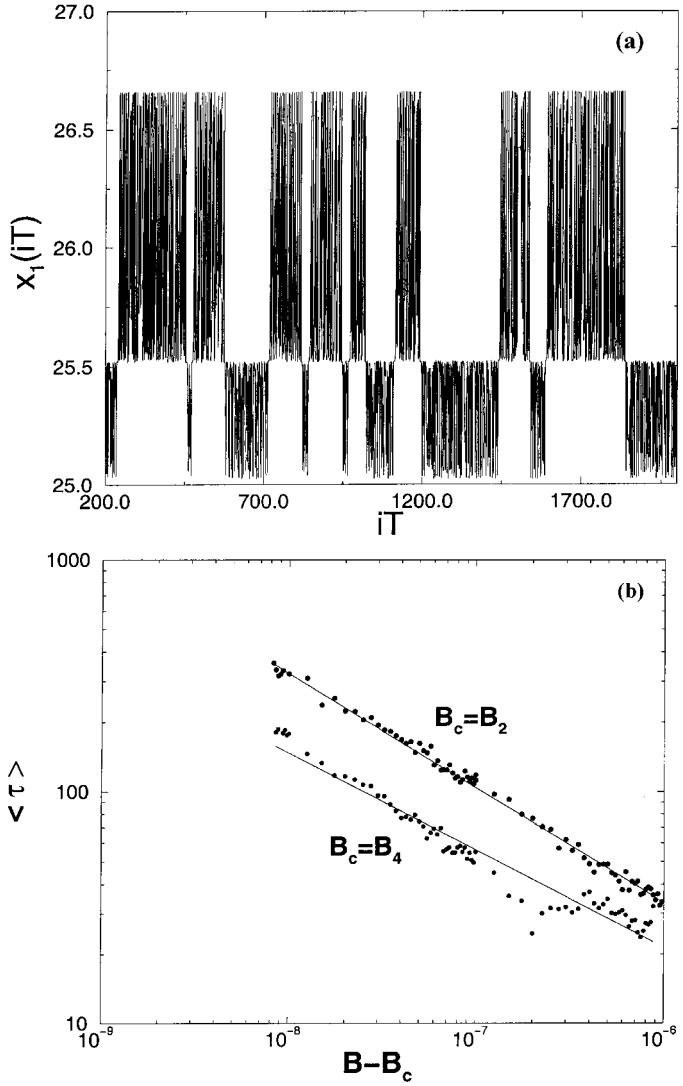

Figure 7. (a) Time series for the stroboscopic map of x_1 with $W = 3.2W_0$ and B slightly above B_2, showing how the trajectory visits each one of the chaotic bands existing before the band merging. Only the lower branch is shown. (b) Average time between chaos-chaos switchings as a function of the differences $B - B_c$, where the crisis parameter may have the values indicated in Figure 5c as B_2 and B_4.

We have focused our attention on two specific dynamic features: firstly, in the neighborhood of a period-9 window embedded in the chaotic region we characterized type-I intermittency, and obtained a scaling law for the average duration of the laminar phase. Second, close to chaotic band-mergings we have found crisis-induced intermittency, and a scaling law for the time between chaotic switchings was obtained. Our results are in close agreement with theoretical predictions for unimodal maps. The possibility of representing the dynamics of the laser diode by a unimodal map strongly suggests the utility of such lasers as an attractive chaotic generator for information transmission, since the available methods for encoding information in chaos [16, 17] require a partition of the phase space (to associate each side of partition with a binary symbol). In the case of unimodal maps, the extremum of the map allows for a natural

partition, and the symbolic dynamics (the grammar) can be readily determined. Moreover, methods for controlling chaos such as the OGY method can be more easily implemented in one-dimensional systems [18]. Results on the implementation of this method in the laser model here studied will be published elsewhere [19].

Acknowledgments

This work was made possible through a partial financial support from the following Brazilian government agencies: CNPq (with NSF-INT through an International cooperation program), CAPES, and FAPESP.

References

1. Ciofini, M., Labate, A., Meucci, R., and Arecchi, F. T., 'Experimental control of chaos in a delayed high-dimensional system', *European Physical Journal D* **7**, 1999, 5–9.
2. Kawaguchi, H., 'Optical bistability and chaos in a semiconductor laser with a saturable absorber', *Applied Physics Letters* **45**, 1984, 1264–1266.
3. Winful, H. G., Chen, Y. C., and Liu, J. M., 'Frequency locking, quasiperiodicity, and chaos in modulated self-pulsing semiconductor lasers', *Applied Physics Letters* **48**, 1986, 616–618.
4. Wang, G., Nagarajan, R., and Tauber, D., 'Reduction of damping in high-speed semiconductor lasers', *IEEE Photonics Technology Letters* **5**, 1993, 642–645.
5. Bennet, S., Snoweden, C. M., and Iezekiel, S., 'Effect of negative gain suppression on the stability of laser diodes', *Applied Physics Letters* **66**, 1995, 1874–1876.
6. Van Wiggeren, G. D. and Roy, R., 'Communication with chaotic lasers', *Science* **279**, 1998, 1198–1200.
7. Figueiredo, J. C. B. and Malta, C. P., 'Lyapunov graph for two-parameters map: Application to the circle map', *International Journal of Bifurcation and Chaos* **8**, 1998, 281–293.
8. Romeiras, F., Grebogi, C., and Ott, E., 'Critical exponents for power-spectra scaling at mergings of chaotic bands', *Physical Review A* **38**, 1988, 463–468.
9. Eckmann, J. P. and Ruelle, D., 'Ergodic theory of chaos and strange attractors', *Reviews of Modern Physics* **57**, 1985, 617–656.
10. Bohr, T., Bak, P., and Mogens, H. J., 'Transition to chaos by interaction of resonances in dissipative systems. II. Josephson junctions, charge-density waves, and standard maps', *Physical Review A* **30**, 1984, 1970–1981.
11. Ding, E. J., 'Analytic treatment of a driven oscillator with a limit cycle', *Physical Review A* **35**, 1987, 2669–2683.
12. Metropolis, N., Stein, M. L., and Stein, P. R., 'On finite limit sets for transformations on the unit interval', *Journal of Combinatorial Theory* **15**, 1973, 25.
13. Pomeau, Y. and Manneville, P., 'Intermittent transition to turbulence in dissipative dynamical systems', *Communications in Mathematical Physics* **74**, 1980, 189–197.
14. Grebogi, C., Ott, E., and Yorke, J. A., 'Crises, sudden changes in chaotic attractors, and transient chaos', *Physica D* **7**, 1983, 181–200.
15. Grebogi, C., Ott, E., Romeiras, F., and Yorke, J. A., 'Critical exponents for crisis-induced intermittency', *Physical Review A* **36**, 1987, 5365–5380.
16. Hayes, S., Grebogi, C., and Ott, E., 'Communicating with chaos', *Physical Review Letters* **70**, 1993, 3031–3034.
17. Hayes, S., Grebogi, C., Ott, E., and Mark, A., 'Experimental control of chaos for communication', *Physical Review Letters* **73**, 1984, 1781–1784.
18. Shinbrot, T., Ott, E., Grebogi, C., and Yorke, J. A., 'Using chaos to direct orbits to targets in systems describable by a one-dimensional map', *Physical Review A* **45**, 1992, 4165.
19. Manffra, E. P., Caldas, I. L., and Viana, R. L., 'Controlling chaos in a self-pulsating laser diode model', submitted for publication.